1966

Similitude requirements for models of a vortex tube

Mervin Leroy Smith
Iowa State University

SIMILITUDE REQUIREMENTS FOR MODELS OF A VORTEX TUBE

by

Mervin Leroy Smith

A Dissertation Submitted to the
Graduate Faculty in Partial Fulfillment of
The Requirements for the Degree of
DOCTOR OF PHILOSOPHY

Major Subject: Theoretical and Applied Mechanics

Approved:

Signature was redacted for privacy.
In Charge of Major Work

Signature was redacted for privacy.
Head of Major Department

Signature was redacted for privacy.
Dean of Graduate College

Iowa State University
Of Science and Technology
Ames, Iowa

1966

TABLE OF CONTENTS

INTRODUCTION

The vortex tube - frequently referred to as the Ranque - Hilsch vortex tube - has been investigated both experimentally and theoretically by many researchers for a number of years. The device enjoys continued investigation for two reasons: it's considerable academic interest because of the difficult non-linear differential equations which describe the complicated flow pattern within the tube and also, the possibility of practical application is intriguing because of the extreme simplicity of fabrication and operation (i.e., it requires no moving parts). Theoreticians, however, have achieved only marginal success. The experimentalists have determined temperature, pressure, velocity profiles within the tube and made some optimization studies. The need for a study based on the principles of similitude, if practical, is long overdue and is the purpose of this paper. By the very nature of similitude, such a study should be of both academic interest (i.e., if the variables are identifiable, then similitude will provide a systematic, efficient approach to the investigation of their dependence) as well as of practical interest because of the automatic production of design and operating conditions.

The present investigation was restricted to a phenomenological study of the effects on the temperature of the exhaust air (at the cold exits of a pair of tubes exhibiting geometrical similarity) due to variations of inlet and cold outlet pressures and flow rates.

The specific questions to be considered are can pertinent, gross-effect variables (i.e., variables descriptive of phenomena exterior of the vortex chamber and tube irrespective of detailed interior flow and heat transfer phenomena) be identified to a degree admitting the prediction of prototype temperatures given model temperatures and, if so, is true or distorted model theory required.

SUMMARY OF PREVIOUS WORK

The theory and operation of the vortex tube has been considered by many investigators dating back to the mid-thirties. M. G. Ranque discovered the thermal separation capabilities of the vortex tube and received a French patent in 1933 and an American patent a year later. Except for the patents, Ranque's work apparently remained unrecognized until World War II when its first application evolved as a refrigerating device for the experimental German rocket plane. The first detailed publication, R. Hilsch (2), appeared after the war and reported some optimization studies relative to tube geometry and inlet gas pressure as well as a qualitative description of the flow in the vortex tube. As initial conjectures relative to a theoretical explanation of the thermal separation phenomenon, he postulated a radially outward flow of kinetic energy due to internal friction. Since the Hilsch article, the literature has naturally divided into three separate categories:

1. Experimental
    - A. Optimization studies
    - B. Detailed temperature, pressure, velocity profiles
2. Theoretical
3. Application

Applications to date have been limited in number. The device has recently (15) been utilized by the New York Central Railroad as a drinking water cooler (since they would naturally have a quantity

of compressed air available). Another (3) is used as a cooling device for a dew point meter. The feasibility of using a vortex tube to contain a fissioning gas has been demonstrated by Keyes (4). The possibility of obtaining higher propellent temperatures in a nuclear rocket than could be obtained by the reactor alone has been suggested by Deissler and Perlmutter (1). A recent article (15) discusses the design of personal air-conditioning units for protective clothing. It may be seen that the range (if not the number) of applications is rather significant. Due to the extreme simplicity of this device, it may be supposed that many more future applications will be found.

An excellent bibliography of vortex tube literature, with abstracts, exists for the period extending from Ranque's patent through 1953 in the form of a paper by Westley (17). A brief examination of this report will show that interest waxed and waned during this period. However, interest has remained relatively high for the past several years probably due to the fact, as Westley (17) expressed it, that "Besides its possible importance as a practical device, the vortex tube presented a new and intriguing phenomenon in fluid dynamics."

Parametric studies of variations of average output temperatures with tube geometry and input pressure have been reported by Martynovskii and Alekseev (7). Some conclusions were:

1. That a dual tangential trough input resulted in the greatest temperature difference,

2. that best efficiency was obtained when the diameter of the hot tube and vortex chamber were the same,

3. a central, circular, cold orifice in a flat diaphragm produced greatest temperature differences,

4. the optimum ratio of hot tube diameter to cold orifice diameter was in the range 1.85 to 1.95,

5. for the input pressure ranges used (2 to 10 atmospheres), a variation of input gas stagnation temperature from 7°C to 25°C caused no measurable effect on the output temperature differences (hot exit - cold exit).

These conclusions were considered in the design of the tubes used in the present work.

A concise summary of the state of developement of the theory of the vortex tube in 1959 is given by F. Kreith in the 'Discussion' section of a paper by Lay (6). Theories up to this time had ranged from simple adiabatic cooling through a centrifugally generated pressure gradient, through a suggestion that the vortex tube cooling and heating phenomena was due to an ultrasonic effect, and finally, to a two dimensional, compressible, turbulent flow model. A recent extension of this latter model has been given by Sibulkin (11, 12, 13), and will be outlined here. Sibulkin (13) notes that "The description of the vortex tube gives rise to a steady-flow problem in three-dimensional space which is mathematically intractable." He has, therefore, chosen as model an unsteady, two-dimensional problem by neglecting the shear forces associated with the axial and radial

components of the velocity in comparison to the shear associated with the circumferential velocity distribution. A perfect gas and a Mach number much less than one are assumed. Under these assumptions, Sibulkin (11, 12) has shown that the Navier-Stokes and energy equations can be reduced to

$$\rho r \omega^2 = \frac{\partial P}{\partial r} \tag{1}$$

$$\frac{\partial \omega}{\partial T} = \frac{\nu}{r^3} \frac{\partial}{\partial r} \left(r^3 \frac{\partial \omega}{\partial r} \right) \tag{2}$$

$$c_p \frac{\partial T}{\partial t} + \frac{\partial}{\partial t} \left(\frac{v^2}{2} \right) = \frac{1}{\rho} \frac{\partial P}{\partial t} + \frac{\nu}{r} \frac{\partial}{\partial r} \left[r^3 \frac{\partial}{\partial r} \left(\frac{\omega^2}{2} \right) \right] + \frac{K}{\rho r} \frac{\partial}{\partial r} \left(r \frac{\partial T}{\partial r} \right) \tag{3}$$

The left hand side of the latter equation is the rate of change of total enthalpy of a fluid element in the hot tube. The first term on the right is the increase in enthalpy due to compression of a fluid element. The second term on the right is the viscous work on an element. The last term on the right is the net heat conducted into an element. Some conclusions of the Sibulkin (13) paper are:

1. Confirmation of the axial flow pattern of (9) as Figure 1,
2. greatest temperature difference (inlet - cold exit) occurs for smallest cold orifice,
3. the height of the (rectangular) inlet nozzle was found to be a significant geometrical parameter affecting performance -

as the height increased, the core diameter decreased, and the temperature differences increased,

4. general (qualitative) agreement with theoretical and experimental temperature, pressure profiles.

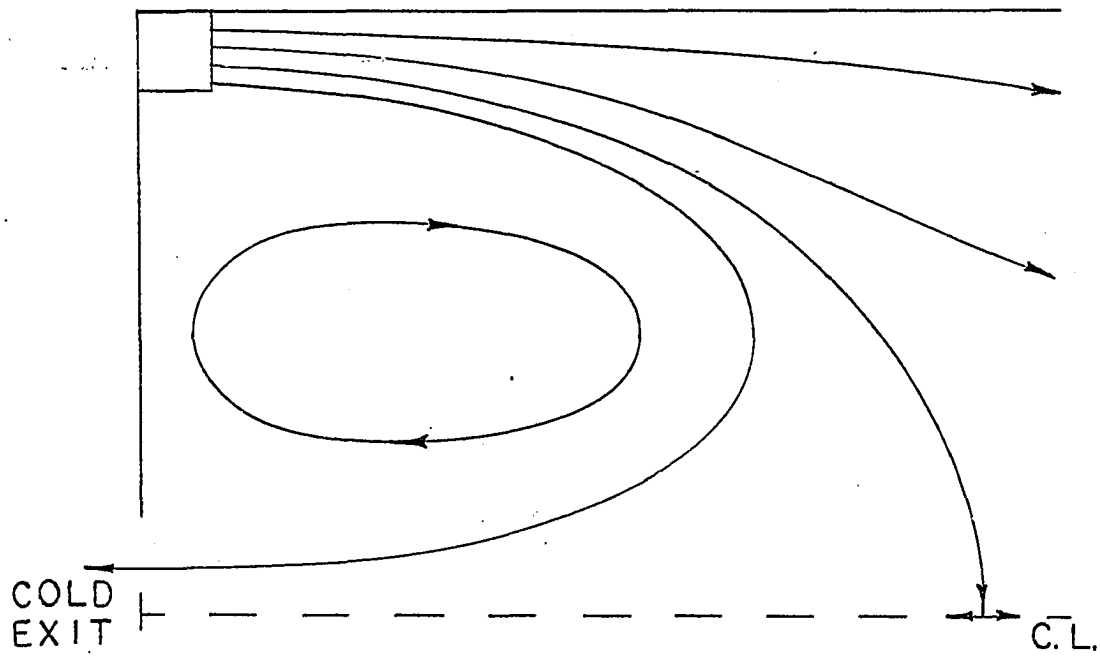

Figure 1. Axial flow pattern

Takahama (14) has recently reported on theoretical and experimental studies made with the object of obtaining formulae for profiles of velocity, temperature, and energy of the air flow which do not include such generally unknown quantities as radial velocity and turbulent diffusivity. Good agreement is achieved between theory and experiment for velocity profiles. However, the experimental temperature profile is of a different form than that of the theoretical

profile, though less different than when compared with previous theories.

In summary, then, the air entering the tangential nozzles creates a circumferential flow distribution in the hot tube moving away from the inlet plane. Considering the entire cross section of the tube, one observes a temperature distribution with a minimum at the center and a maximum near the wall. Qualitative agreement with experiment is achieved when one assumes the net rate of change of total temperature of a fluid element as it spirals toward the center as due to three causes:

1. Turbulent heat transfer into the element as a result of a temperature gradient (conduction),
2. turbulent heat transfer into the element as a result of a pressure gradient (convection), and
3. turbulent shear work done on the element.

Visual inspection techniques have determined that the flow in the tube divides into two rather distinct patterns:

1. A relatively quiescent core centered on the tube axis (the cooler flow on escape), and
2. a high velocity annulus (the warmer flow).

As indicated by the preceding discussion, previous investigations of vortex tubes have been directed specifically toward achieving an explanation of the fundamental fluid phenomenon in such tubes or toward attempts to discover, for a particular tube, those values of the operating parameters which would produce the greatest temperature

difference. No previous work was found which applied similitude theory to the vortex tube system. Due to this total lack in the field, the current work is a pioneering investigation and will proceed by utilizing dimensional analysis to discover significant π terms which are required in the theory of similitude.

DIMENSIONAL ANALYSIS

The first step in the similitude approach is the application of dimensional analysis to the problem. Dimensional analysis, however, assumes the pertinent variables and their dimensions are known. The procedure is to assume a set of variables (with their respective dimensions) and test their validity via the results. Those variables assumed appropriate for the present work are listed in Table 1.

These indicate three types of variables are necessary. They must specify the geometries of prototype and model, dynamics of prototype and model, and those properties of the materials upon which the characteristic phenomena of interest depend.

Geometric Variables

The choice of geometric variables is governed to some extent by the particular style of tube employed. Vortex tubes reported in the literature differ in size, type of vortex chamber (i.e., the inlet air stream may be directed along a normal or otherwise tangent to the vortex tube), the number of such inlets, and the shape (circular, rectangular) of the cross section of the inlet(s). For the present work a dual inlet (shown in Figure 2) was chosen and designed to bring the flow into the vortex chamber in such a way that the flow per channel could be fed into the chamber gradually over an angular range of 180°. Together, the two channels produce a 360° feed. It was felt that this system would result in a lower turbulence

Table 1. Significant variables

Symbol	Definition
d_h	Internal diameter of vortex tube
d_c	Diameter of cold orifice
h	Height of inlet channels
w	Width of inlet channels
l	Length of vortex tube
a	Width of throttle valve slots
T_c	Temperature at cold orifice
T_i	Temperature at inlets
P_c	Pressure at cold orifice
P_i	Pressure at inlets
Q_c	Flow rate from cold orifice
Q_i	Flow rate (total) to inlets
μ	Viscosity of inlet gas
K	Thermal conductivity of inlet gas
K_p	Thermal conductivity of tube material
C_p	Specific heat of gas at constant pressure
C_v	Specific heat of gas at constant volume
α	Moisture content of inlet gas

Figure 2. Photograph of assembled 3/4 inch vortex tube and vortex chamber of 1 inch tube

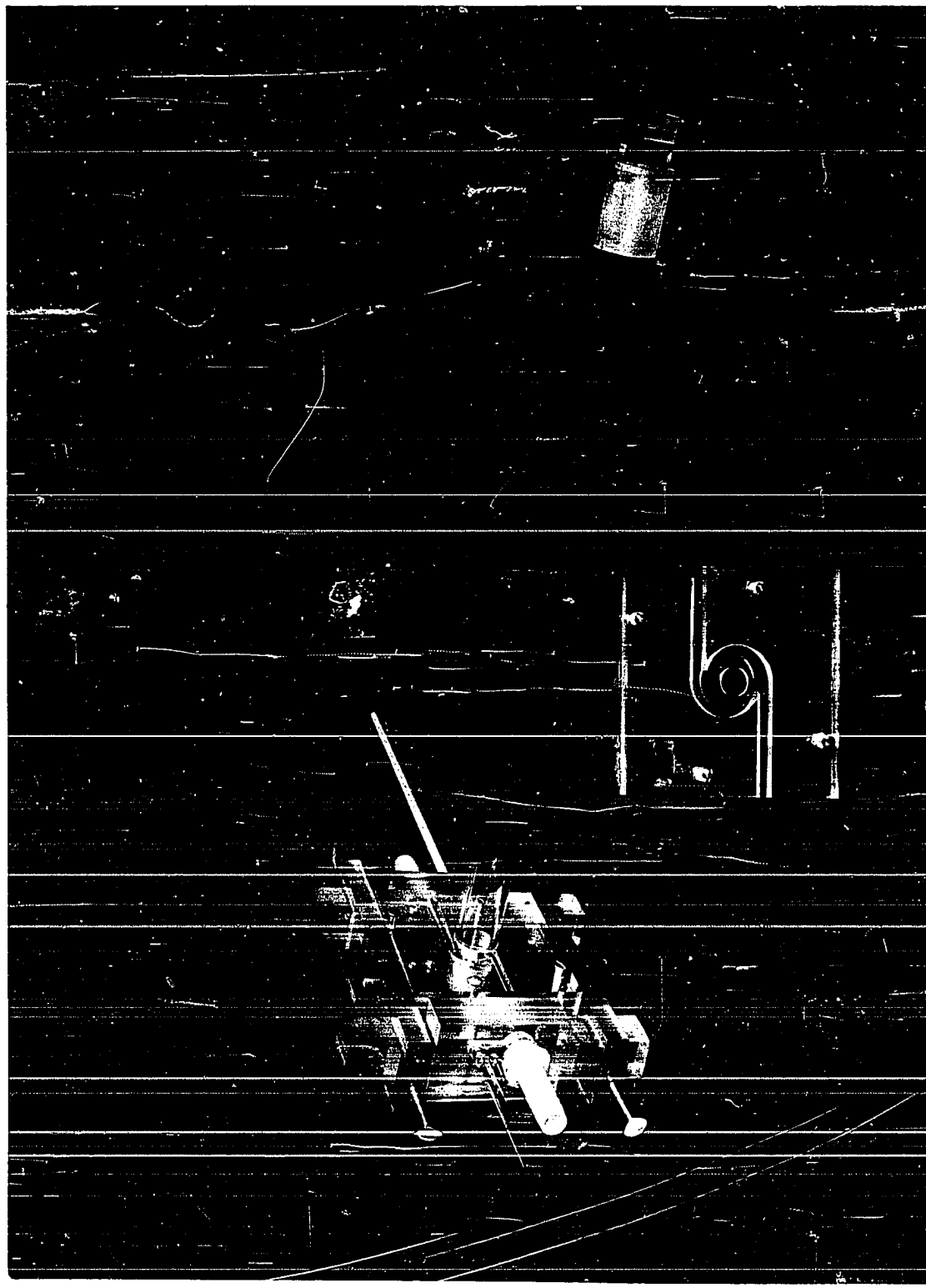

within the chamber (a desirable situation since the cold flow exits along the tube axis from the chamber) than that known to exist in the simple design with single entry via a normal tangent.

Hilsch (2) has shown that larger temperature reductions may be obtained with larger vortex tubes (for a given inlet pressure). However, in the same paper it is shown that the optimum (in the sense of largest temperature difference between hot and cold outlets) ratio of vortex tube diameter to inlet diameter (assuming a circular inlet) is approximately four. Therefore, for optimum performance, d_h is limited by the flow rate available.

The choice of value of d_c depends on whether it is desired to attain very low temperatures or to produce large quantities of cold air. Martynovskii and Alekseev (7) have reported that two is a useful compromise value of the ratio of d_h to d_c.

Sibulkin (13) is apparently the only investigator thus far to have considered rectangular inlet nozzles (others being circular). He concluded that, of the geometrical parameters involved, h was the most significant in determining the temperature of the cold gas stream. The hypothesis supposes that the larger h, the smaller the core and the faster its rotation so that the core should do more work on the annulus and thereby experience an increased temperature drop.

The inlet width w is a determining factor for the flow rate.

Whatever theoretical explanation of the vortex tube evolves, some time (and hence, some length of tube) will be required for the energy separation between the air of the axial region and that of the annulus.

Since the vortex flow configuration near the end of the vortex tube will necessarily be disturbed because of the presence of the throttle valve slots, the number, location (immediately before the end plug), and width a, have been modeled in order to cause as nearly similar disturbance in model and prototype as possible.

The numerical values of these variables is given in Appendix A. Except for d_c all pertinent lengths will henceforth be abbreviated to λ_i. Reference to Figure 3 indicates the above length variables to be independent.

Dynamic Variables

The well - known physical equations which govern fluid flow, viz., the Navier - Stokes equation, the continuity equation, the energy equation, and the equation of state define the variables involved in the description of the internal fluid flow. These variables are pressure, temperature, density, velocity, and acceleration. Under steady state conditions acceleration (whether gravitational or other) would not be expected to be of any significance since measurement of the variables was external to the vortex flow. The density will similarly be excluded - it would form a dependent set with pressure and temperature when the perfect gas law is applied.

The static temperature at the cold exit, T_c, is the quantity to be predicted.

The static temperature at the inlet should be included since

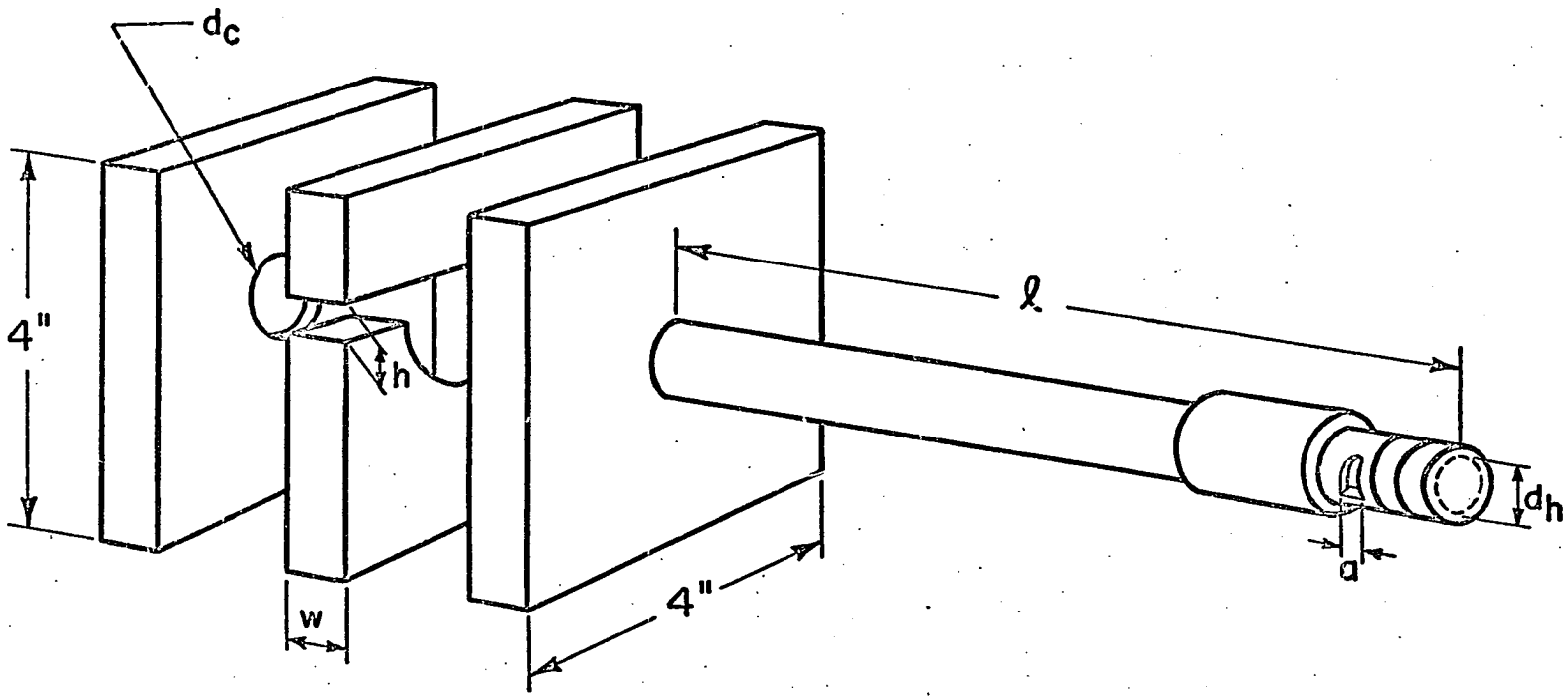

Figure 3. Vortex tube and chamber, exploded view

small changes in this variable produce similar changes in T_c.

The static pressure at the inlet, P_i, is a controlling factor determining flow rate through the tube. For the present investigation, the cold outlet temperature will be shown to be not directly dependent on P_c, but rather on the ratio P_i/P_c and hence, the ratio will be taken as a significant variable rather than the pressures individually.

Various investigators from Hilsch to Takahama have noted the temperature dependence at the cold exit on the mass flow rates which, of course, are relatable to the flow rates Q_i and Q_c through the pressures and temperatures.

Properties of the Materials

Of the three types of variables, those defining properties of the materials of significance to the phenomena in question are frequently the most difficult to decide. This condition results from the fact that a property of significance in one range of operation may be of quite negligible significance in another. The solution, of course, is to test as wide a range of values of the variables as possible.

As noted for the dynamic variables, the four governing equations for fluid flow will supply initial estimates of significant properties of the materials.

The laminar viscosity μ and thermal conductivity K of the inlet gas have been included. Some theorists (e.g., Deissler and Perlmutter (1))

incorporate turbulent viscosity and conductivity for the vortex flow within the tube, and, in fact, the Reynolds number has been estimated in the current inlet channels to be approximately 10,000 (i.e., in the low turbulent region). However, for the length of channel involved here (approximately 2 inches), it is supposed that viscous and heat flow effects should be largely restricted to the laminar boundary layer (5, 10).

Also, the specific heats and moisture content of the inlet gas have been included.

Construction of π Terms

Collecting the previously listed variables, it may be assumed that

$$T_c = F(T_i, d_c, \lambda, P_i/P_c, Q_i, Q_c, \mu, K, K_p, C_p, C_v, \alpha). \quad (4)$$

Assuming a mechanical energy - heat energy interchange within the tube (as Sibulkin (13) suggests), the variables may be assumed to have the following dimensions (see Murphy (8), page 193).

$$d_c \doteq \lambda \doteq L$$
$$T_c \doteq T_i \doteq \Theta$$
$$Q_c \doteq Q_i \doteq L^3T^{-1}$$
$$\mu \doteq FTL^{-2}$$
$$K \doteq K_p \doteq FT^{-1}\Theta^{-1}$$
$$C_p \doteq C_v \doteq L^2T^{-2}\Theta^{-1}$$
$$\alpha \doteq P_i/P_c \doteq 1$$

The symbol $\doteq$ indicates dimensional equality but not necessarily

numerical equality. Therefore, according to the π - Theorem of Dimensional Analysis, there are

$$13 - 4 = 9$$

π terms required. A possible set is

$$\frac{T_i}{T_c} = F\left(\frac{\lambda_i}{d_c}, \frac{\mu C_p}{K}, \frac{C_p}{C_v}, \frac{K_p}{K}, \alpha, \frac{P_i}{P_c}, \frac{Q_i}{Q_c}, \frac{Q_i^2}{C_p T_i d_c^4}\right) \qquad (5)$$

This set is independent since each π term contains one variable which is not utilized by any oth · term.

SIMILITUDE TREATMENT OF PROBLEM

After dimensional analysis has been employed to deduce a set of dimensionless parameters descriptive of the phenomena in question, the theory of similitude may be applied in order to relate these parameters to a prototype-model pair. This involves identification of π terms with model and prototype and deductions concerning relationships among the corresponding variables.

Development of Prediction Equation

A fundamental assumption of similitude is that the form of the equations are the same in model and prototype. Specifically, if Equation 5 is properly descriptive of the prototype, then an expression similar in form is also descriptive of a suitably designed model. Specifically, the following expression may be formed on the basis of Equation 5:

$$\frac{\frac{T_i}{T_c}}{\frac{T_{im}}{T_{cm}}} = \frac{F\left(\frac{\lambda_i}{d_c}, \frac{\mu C_p}{K}, \frac{C_p}{C_v}, \frac{K_p}{K}, \alpha, \frac{P_i}{P_c}, \frac{Q_i}{Q_c}, \frac{Q_i^2}{C_p T_i d_c^4}\right)}{F\left(\frac{\lambda_{im}}{d_{cm}}, \frac{\mu_m C_{pm}}{K_m}, \frac{C_{pm}}{C_{vm}}, \frac{K_{pm}}{K_m}, \alpha_m, \frac{P_{im}}{P_{cm}}, \frac{Q_{im}}{Q_{cm}}, \frac{Q_i^2{}_m}{C_{pm} T_{im} d_{cm}^4}\right)} \tag{6}$$

where the subscript m defines the particular variable as relative to the model. It may be observed that if all homologous π terms on the right hand side of this expression are equal, there results

$$\frac{T_i}{T_c} = \frac{T_{im}}{T_{cm}} \tag{7}$$

which is known as the prediction equation because of its ability to predict prototype behavior (the left hand side) given the model behavior. This equation, moreover, indicates a true model. It should be noted, however, that if not all homologous π terms may be set equal, then a distortion exists and Equation 7 may not be valid. In that event a more realistic prediction equation is

$$\frac{T_i}{T_c} = \delta \frac{T_{im}}{T_{cm}} \tag{8}$$

where δ is a prediction factor to be determined and whose purpose is to account for the lack of satisfaction of the particular distorted π terms. Depending on the problem and the variables specified, δ may vary from a constant to a function of all π terms.

Design Conditions

Identification of homologous terms of Equation 6 leads to the following design conditions.

$$\frac{\lambda_i}{d_c} = \frac{\lambda_{im}}{d_{cm}} \tag{9}$$

these imply the length scale (relating model and prototype):

$$\frac{\lambda_i}{\lambda_{im}} = \frac{d_c}{d_{cm}} = n \tag{10}$$

This expression states the need for geometrical similarity of model and prototype and was a governing factor in prototype and model fabrication. The next three design conditions relate to properties of the materials:

$$\frac{\mu C_p}{K} = \frac{\mu_m C_{pm}}{K_m} \tag{11}$$

$$\frac{C_p}{C_v} = \frac{C_{pm}}{C_{vm}} \tag{12}$$

$$\frac{K_p}{K} = \frac{K_{pm}}{K_m} \tag{13}$$

The easiest way to satisfy these restrictions on the properties of the gas and tube material is to use the same gas in model and prototype (air in the current work) and the same construction materials (Plexiglas, here). Because of temperature and pressure variations the equality, in practice, is approximate. However, the approximation is a very good one for air. Next

$$\alpha = \alpha_m \tag{14}$$

This requirement stipulates the same moisture content (preferably none) in the gas used in model and prototype. Since the local campus air supply equipment incorporates an after-cooler, no attempt was made to control this parameter except that each prototype-model data set was obtained as rapidly as possible in order to minimize possible variations of α if any moisture should escape extraction.

Operating Conditions

The remaining equivalences stipulate the operating conditions.

$$\frac{P_i}{P_c} = \frac{P_{im}}{P_{cm}} \tag{15}$$

$$\frac{Q_i}{Q_c} = \frac{Q_{im}}{Q_{cm}} \tag{16}$$

That is, temperature ratios for prototype and model should be comparable only for those situations in which the pressure and flow ratios are equal. Finally

$$\frac{Q_i^2}{C_p T_i d_c^4} = \frac{Q_{im}^2}{C_{pm} T_{im} d_{cm}^4} \tag{17}$$

or equivalently

$$\left(\frac{Q_i}{Q_{im}}\right)^2 = \left(\frac{C_p}{C_{pm}}\right)\left(\frac{T_i}{T_{im}}\right)\left(\frac{d_c}{d_{cm}}\right)^4 \tag{18}$$

But in practice

$$C_p \approx C_{pm}$$
$$T_i \approx T_{im}$$

Therefore

$$\frac{Q_i}{Q_{im}} = n^2 \quad \text{(approximately)} \tag{19}$$

This represents an operating condition on the flow magnitudes, and

also, since

$$\frac{Q_i}{Q_{im}} = \frac{Q_c}{Q_{cm}} \quad \text{by Equation 16}$$

There results the following condition on the cold flows

$$\frac{Q_c}{Q_{cm}} = n^2 \quad \text{(approximately)} \qquad (20)$$

Experimental Procedure

The restrictions on flow magnitude developed as the most difficult of the design and operating conditions to satisfy. It may be noted that for length scales as large as two, the flow rates in the prototype must be approximately four times those in the model. Depending on the range of flow rates to be investigated, this feature can lead to rather serious requirements on the range of the rotameters. However, within the attainable range, the experimental procedure evolved (for a single gas and tube material) into the following technique (see Figure 4 for a schematic of the system and Appendix A for a listing of test equipment).

The range of operation of the system which would allow approximate satisfaction of the operating conditions was determined and an error analysis made on the test equipment (see Appendix B). In view of the range, the error analysis, and difficulty with satisfying the operating condition relative to flow magnitudes (to be discussed later under Results), it was decided that for the acquisition of

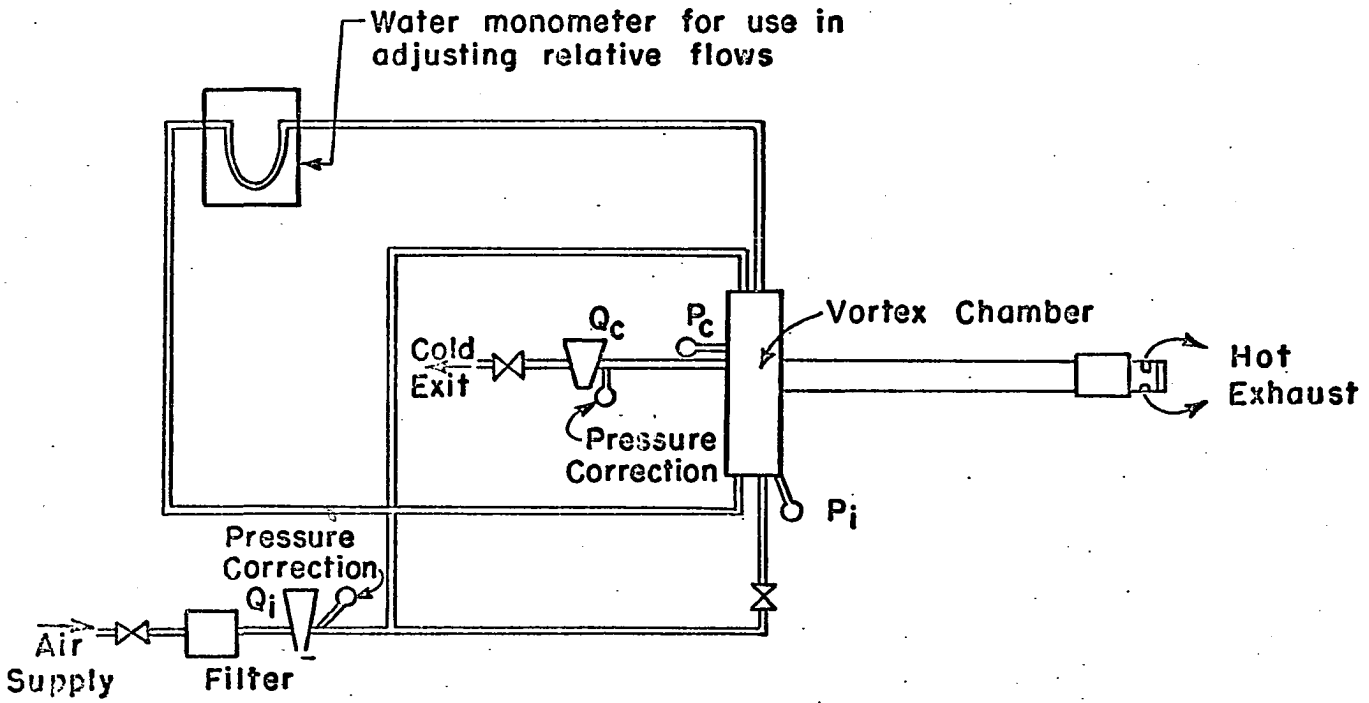

Figure 4. Schematic of test apparatus

raw data the pressure ratio should be considered a parameter and set at four different values. For each value of the pressure ratio, those hot valve, cold valve, and inlet valve settings were obtained which simultaneously produced the desired pressure ratios and a minimum observable reading ($Q_c > 2CFM$) on the cold flow rotameter. This condition of operation produced the coldest temperature of the cold flow obtainable for that given pressure ratio. In order to minimize the several minutes required to overcome the thermal inertia of the system once the above conditions were set, the inlet valve was opened an additionally small amount. This had the effect of raising the pressure ratio and lowering the cold flow temperature still more.

After a few minutes the inlet valve was again adjusted to reset the pressure ratio at the desired value. Thermometer and rotameter data were recorded after two successive readings of the thermometer (separated by at least one minute) detected not more than a $0.2^{\circ}F$ change (the estimation limit was $0.1^{\circ}F$). The inlet valve was then closed a small amount in order to lower the pressure ratio and raise the cold flow temperature somewhat. The inlet valve was then reset to produce the desired pressure ratio and the temperature and flows were again recorded as before. The averages of these temperatures and flows were taken as the best estimate of the first data point for a given pressure ratio.

The next data point was obtained similarly. Hot, cold, and inlet valves were adjusted slightly so as to raise the cold flow rotameter reading (while maintaining the pressure ratio) which, as

before, allowed a temperature measurement to be taken under an increasing temperature condition. Then the inlet valve was closed slightly to raise the temperature, then reset to its desired position, and a temperature recorded in a decreasing temperature condition. This set was then averaged for the second graph point. After a complete set of decreasing temperature and flow ratio points were recorded, the set was spot-checked by obtaining two to four more points taken in a reverse operation from that described above, i.e., starting with the flow ratio near one and retracing the cycle back to the minimum cold flow configuration.

The first model-prototype pair constructed were the previously mentioned one inch diameter tube and a 1/2 inch diameter tube. It was discovered, however, that although both tubes functioned within the range of the rotameters for comparable pressure ratios, the 1/2 inch tube flows were near the lower limits of the rotameters and considered unreliable. Also, the flow ratios obtainable were quite small (i.e., near one). Hence, 1/2 inch tube data will not be included in the general results, although observations of gross effects will be noted occasionally.

The 3/4 inch tube was constructed in order to place the rotameter measurements nearer mid-scale.

RESULTS

As previously mentioned, a problem encountered early in the operation of the system was the satisfaction of the operating conditions determining flow magnitudes. It was found that for three different size tubes of diameters 1 inch, 3/4 inch, and 1/2 inch the flow ratios of prototype to model were all somewhat greater than n^2 when the operating condition on the pressure ratios was satisfied.

At first glance the flow condition appears redundant in that if geometry, fluid, pressure, and temperature are fixed, then the flow should be determined. In practice, however, there is some distortion of model due to the omission of a length variable characteristic of the inlet region of the channels and descriptive of flow contraction at these locations. This effect would be relatively more severe for the smaller inlets and would tend to increase the effective area ratios over the channel area ratios. This omission was not thought of serious significance and allowed some simplification of fabrication. It was decided to fix the pressures and record data of temperature and flow for various settings of the throttle valves and account for the above distortion via the resulting prediction factor.

Another observation was that temperature ratios T_i/T_c were sensibly independent of P_c for pressure ratios in the range $1.1 \leq P_i/P_c \leq 1.5$, flow ratios in the range $1 \leq Q_i/Q_c \leq 8$, and for $2 \leq P_c \leq 6$ psig. Hence, for convenience, all subsequent data was obtained with P_c set at 4 psig.

Figures 5 and 6 are graphical representations of a complete set of data for prototype and model respectively (data listed in Tables 2 and 3). Some aspects of these curves agree with the findings of previous experimental investigations, viz., the rapid fall of T_c with initially increasing flow ratio (T_i is practically constant per curve), an apparent minimum T_c depending on the pressure ratio and occurring at larger flow ratios for larger pressure ratios, and a lowering of T_c with increasing pressure ratio for a given flow ratio. However, there is one qualitative aspect which differs appreciably from previously reported investigations (e.g., Westley (17), Martynovskii and Alekseev (7), and Takahama (14)). Current data do not support their observations that temperature ratio versus mass ratio curves pass through a maximum and decline for higher mass ratios. For example, Martynovskii and Alekseev (7) report, for several tube sizes and operating conditions, a minimum value of T_c near a mass ratio of

$$\frac{M_c}{M_i} \approx 0.3.$$

It is the author's opinion that their observations were probably a result of heat conduction from the environment through the cold portions of their apparatus and, of course, all data would be more or less affected by this. The use of Plexiglas for construction material may be supposed to have minimized this effect in the present work (the others referred to used tubes constructed largely of copper).

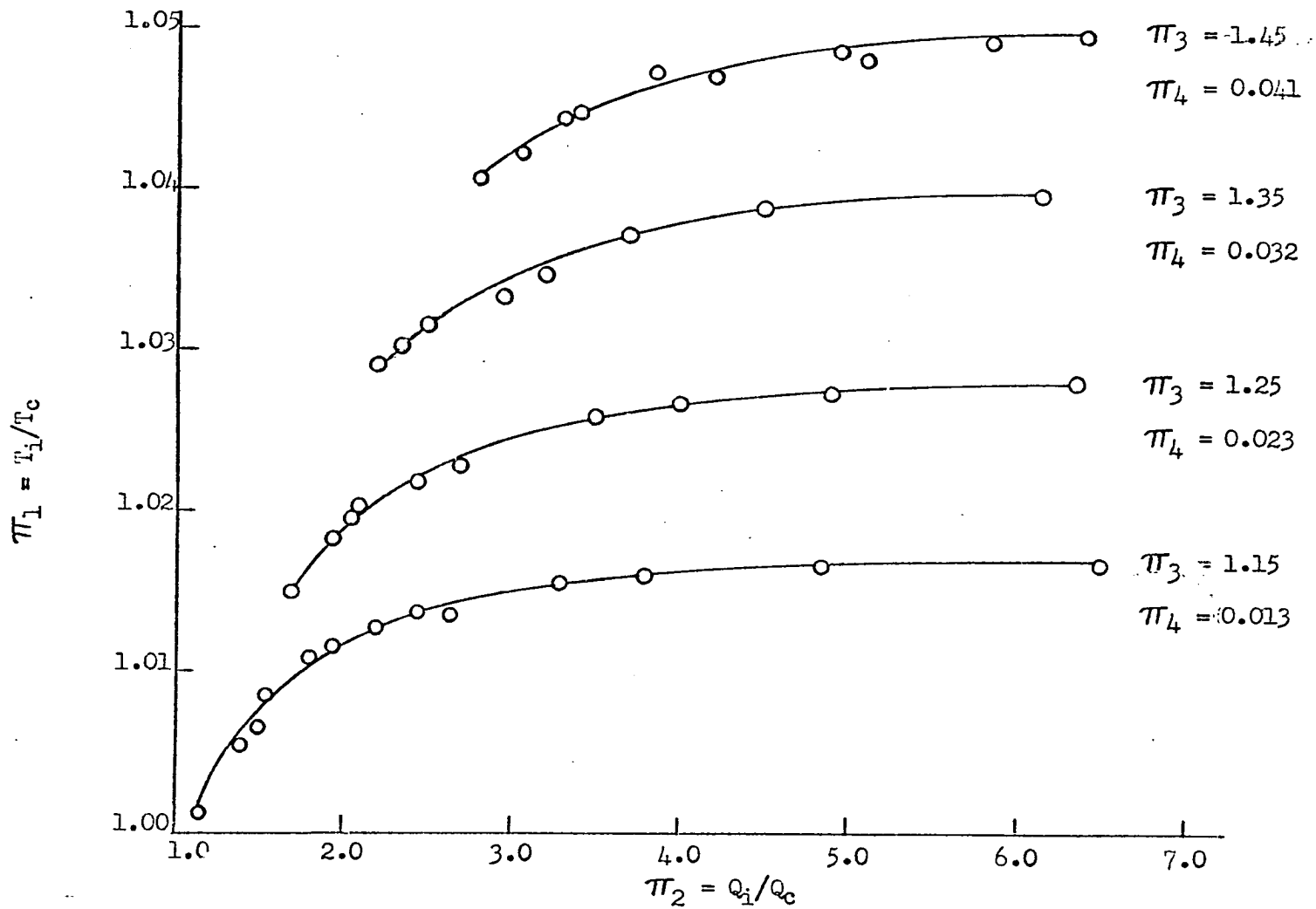

Figure 5. Temperature ratio versus flow ratio. Tube inside diameter = 1.00 inch. Low specific humidity. Parameters: $\pi_3 = P_i/P_c$, $\pi_4 = Q_i^2/C_p T_i d_c^4$.

Table 2. Experimental data for Figure 5

Pressure ratio	Pressure		Flow rate		Temperature	
	P_c psia.	P_i psia.	Q_c ft.^{3}/min.	Q_i ft.^{3}/min.	T_c °F	T_i °F
1.15	18.65	21.45	2.5	21.7	73.3	81.1
			2.5	21.7	73.5	81.2
			3.6	21.7	73.3	81.3
			3.6	21.7	73.5	81.4
			5.2	21.7	73.7	81.5
			5.2	21.7	73.9	81.6
			7.1	21.7	74.6	81.7
			7.1	21.7	74.8	81.8
			9.6	21.7	75.7	81.8
			9.6	21.7	75.8	81.8
			10.7	21.4	76.3	81.9
			10.7	21.4	76.4	82.0
			12.6	21.4	77.3	82.0
			12.6	21.4	77.5	82.0
			13.9	21.1	78.8	82.1
			13.9	21.1	78.8	82.1
			7.9	21.7	75.7	82.3
			7.9	21.7	75.5	82.3
			4.4	21.7	74.5	82.3
			4.4	21.7	74.3	82.4
1.25	18.65	23.30	4.4	28.4	68.5	82.3
			5.7	28.4	68.6	82.4
			7.4	28.4	68.9	82.4
			10.4	28.4	70.4	82.4
			10.6	28.4	70.7	82.3
			12.6	28.4	71.4	82.3
			14.3	28.0	72.8	82.3
			16.0	28.0	73.9	82.3
			8.9	28.4	69.9	82.3
			4.6	28.4	68.5	82.3
1.35	18.65	25.15	5.2	33.8	62.9	82.6
			7.9	33.8	63.6	82.6
			11.5	33.8	65.7	82.7
			15.1	33.8	67.7	82.6
			10.5	33.8	65.3	82.6
			8.6	33.8	64.3	82.7
			6.0	33.8	63.3	82.7
1.45	18.65	27.05	5.9	38.2	58.6	82.9
			7.7	38.2	58.9	82.9
			9.6	38.2	59.6	82.9
			11.8	38.2	60.7	82.8

Table 2 (Continued)

Pressure ratio	Pressure		Flow rate		Temperature	
	P_c psia.	P_i psia.	Q_c ft.^{3}/min.	Q_i ft.^{3}/min	T_c °F	T_i °F
1.45	18.65	27.05	13.6	38.2	62.3	82.8
			11.0	38.2	60.4	82.8
			8.0	38.2	59.3	82.8
			6.6	38.2	58.8	82.8
			6.2	38.2	58.3	82.8

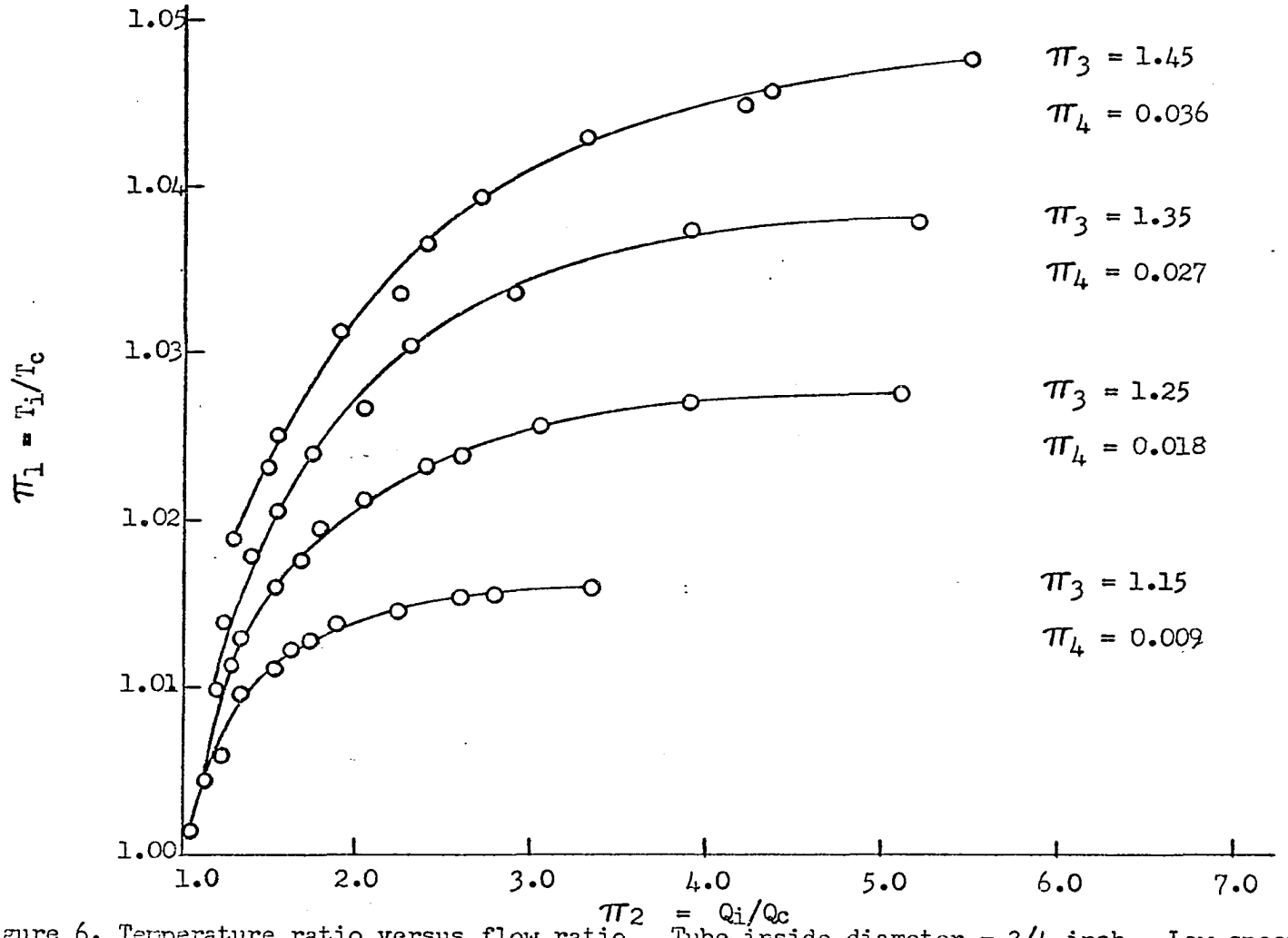

Figure 6. Temperature ratio versus flow ratio. Tube inside diameter = 3/4 inch. Low specific humidity. Parameters: $\pi_3 = P_i/P_c$, $\pi_4 = Q_i^2/C_p T_i d_c^4$.

Table 3. Experimental data for Figure 6

Pressure ratio	Pressure P_c psia.	Pressure P_i psia.	Flow rate Q_c ft.^{3}/min.	Flow rate Q_i ft.^{3}/min	Temperature T_c °F	Temperature T_i °F
1.15	18.65	21.45	3.4	10.4	69.0	76.9
			3.4	10.4	69.5	76.9
			4.4	10.0	70.3	77.2
			4.4	10.0	70.5	77.2
			5.0	10.0	70.9	77.3
			5.1	9.9	71.1	77.3
			6.0	9.7	72.0	77.4
			6.0	9.7	72.1	77.4
			6.6	9.	72.9	77.5
			6.6	9.7	73.0	77.5
			7.5	9.7	74.2	77.6
			7.5	9.7	74.3	77.6
			8.6	9.7	77.4	77.8
			8.6	9.7	77.4	77.8
			5.5	9.7	72.6	78.2
			5.5	9.7	72.6	78.3
			3.9	9.9	71.7	78.4
			3.9	9.9	71.5	78.5
			2.8	10.2	71.3	78.7
			2.8	10.2	71.1	78.8
1.25	18.65	23.30	3.3	14.1	66.5	79.6
			3.3	14.1	66.7	79.7
			4.0	14.1	66.5	79.8
			4.0	14.1	66.7	79.9
			5.1	14.0	67.7	80.0
			5.0	14.0	67.9	80.0
			6.1	13.7	69.0	80.0
			6.1	13.7	69.3	80.1
			7.1	13.7	70.5	80.2
			7.1	13.7	70.7	80.2
			8.8	13.5	72.7	80.2
			8.8	13.1	72.9	80.2
			10.5	13.0	75.1	80.3
			10.5	13.0	75.1	80.3
			5.8	13.8	69.6	80.7
			5.8	13.8	69.4	80.8
			3.1	14.3	67.9	80.9
			2.9	14.1	67.6	81.0
1.35	18.65	25.15	3.1	17.3	62.7	81.5
			3.1	17.3	62.7	81.5
			4.7	17.1	63.3	81.5

Table 3 (Continued)

Pressure ratio	Pressure P_c psia.	Pressure P_i psia.	Flow rate Q_c ft.^{3}/min.	Flow rate Q_i ft.^{3}/min.	Temperature T_c °F	Temperature T_i °F
1.35	18.65	25.15	4.7	17.1	63.6	81.5
			5.9	17.0	64.7	81.5
			5.9	17.0	64.9	81.5
			7.5	17.0	66.7	81.5
			7.3	17.0	66.9	81.5
			9.1	16.7	69.0	81.6
			9.1	16.7	69.2	81.6
			11.2	16.3	72.2	81.7
			11.2	16.3	72.4	81.7
			13.2	16.0	76.0	81.7
			13.2	16.0	76.1	81.7
			6.1	17.0	66.4	82.0
			6.1	17.0	66.2	82.1
			3.1	17.5	64.0	82.2
			3.1	17.5	63.6	82.3
1.45	18.65	27.05	3.05	20.0	58.5	82.8
			3.05	20.0	58.7	82.8
			4.4	20.0	59.0	82.7
			4.4	20.0	59.1	82.6
			6.0	20.0	60.5	82.5
			6.0	20.0	60.7	82.5
			7.0	20.0	62.0	82.5
			7.0	20.0	62.3	82.5
			8.5	19.7	64.4	82.5
			8.5	19.7	64.6	82.5
			10.6	19.5	66.9	82.5
			10.6	19.5	67.0	82.5
			12.5	19.4	70.0	82.4
			12.5	19.4	70.2	82.4
			15.0	18.7	73.8	82.4
			15.0	18.7	73.9	82.4
			8.5	19.7	65.2	82.4
			8.5	19.7	64.9	82.4
			3.9	20.0	60.1	82.6
			3.9	20.0	59.8	82.7

Figure 7 is a superposition of Figures 5 and 6 with data point uncertainty intervals (see Appendix B) shown. Within these intervals the curves are of the same form for each pressure ratio. For a given flow ratio, the magnitudes of the temperature ratios (for a particular pressure ratio) may be observed to be within the uncertainty intervals. The matter of the inequality of the operating condition

$$\frac{Q_i^2}{C_p T_i d_c^4} = \frac{Q_{im}^2}{C_{pm} T_{im} d_{cm}^4}$$

can be of no more than secondary significance since as much as a 35% change of value of this term for corresponding curves of prototype and model still allows curve overlap within the error limits.

Figures 8, 9 and 10 (data listed in Tables 4 and 5) are similar to Figures 5, 6 and 7 except that atmospheric absolute humidity for sets 8 and 9 was somewhat greater than for sets 5 and 6 (38 grains/pound dry air and 34 grains/pound dry air). However, no quantitative conclusions are possible on the question of effect of moisture because actual air line conditions could not be determined. But in all cases there is apparent indication that, for comparable values of the parameters, a lower humidity condition is associated with a lower value of T_c. In the event of cold temperatures below the dew point, it may be supposed the effect could become significant (cf., Lay (6)).

Cursory investigation of the error limits of the data points indicates uncertainty of the value of the flow ratio becomes inordinantly

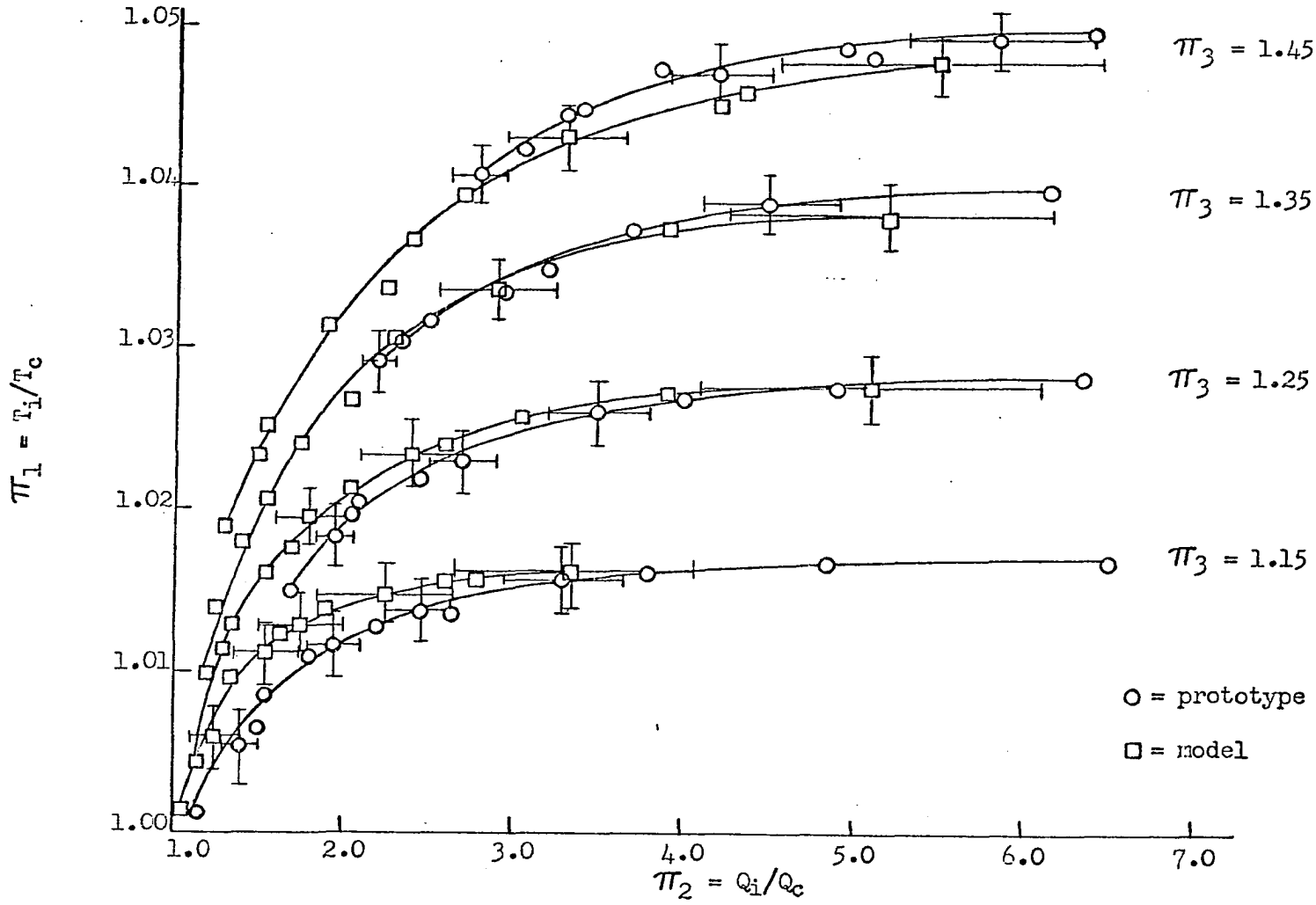

Figure 7. Superposition of prototype (Figure 5) and model (Figure 6). Low specific humidity.

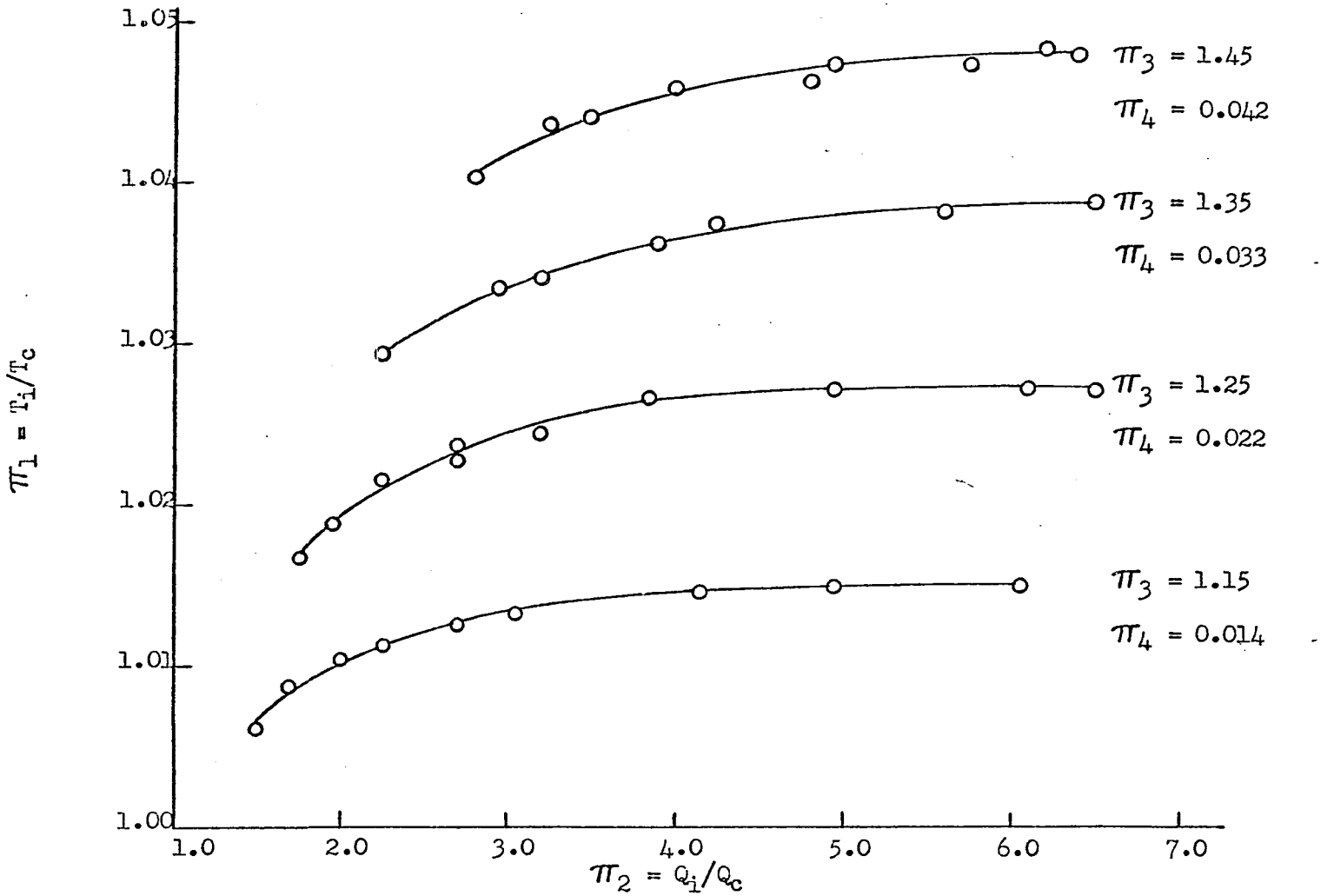

Figure 8. Temperature ratio versus flow ratio. Tube inside diameter = 1.00 inch. High specific humidity. Parameters: $\pi_3 = P_i/P_c$, $\pi_4 = Q_i^2/C_p T_i d_c^4$.

Table 4. Experimental data for Figure 8

Pressure ratio	Pressure P_c psia.	Pressure P_i psia.	Flow rate Q_c ft.^{3}/min.	Flow rate Q_i ft.^{3}/min	Temperature T_c °F	Temperature T_i °F
1.15	18.75	21.60	3.4	21.8	63.0	71.8
			3.4	21.8	63.1	71.7
			4.5	21.8	63.0	71.7
			4.5	21.8	63.1	71.7
			6.6	21.7	63.4	71.6
			6.6	21.7	63.6	71.6
			8.8	21.6	64.5	71.6
			8.8	21.6	64.5	71.7
			9.8	21.3	65.0	71.7
			9.8	21.3	65.1	71.7
			11.8	21.3	66.0	71.7
			11.8	21.3	66.0	71.7
			13.4	21.1	67.2	71.8
			13.4	21.3	67.3	71.7
			15.5	20.7	69.0	71.8
			15.2	20.7	69.1	71.9
			18.0	20.7	71.3	72.0
			18.0	20.7	71.3	72.0
			14.2	20.9	68.8	72.2
			14.2	20.9	68.7	72.2
			10.8	21.4	66.2	72.2
			11.0	21.4	66.0	72.2
			8.0	21.4	65.3	72.3
			8.0	21.4	65.1	72.3
			5.5	21.4	64.1	72.4
			5.8	21.7	64.0	72.4
1.25	18.75	23.40	4.4	27.9	59.5	74.1
			4.4	27.9	59.7	74.1
			5.5	27.9	59.7	74.0
			5.8	27.6	59.9	74.0
			6.9	27.6	60.1	74.0
			6.9	27.6	60.1	74.0
			8.0	27.9	60.4	73.9
			7.7	27.6	60.5	73.8
			10.1	27.9	61.8	73.8
			10.1	27.6	62.0	73.8
			11.2	27.6	62.4	73.8
			11.2	27.6	62.6	73.9
			13.0	27.6	63.3	74.0
			13.0	27.6	63.5	74.0

Table 4 (Continued)

Pressure ratio	Pressure P_c psia.	Pressure P_i psia.	Flow rate Q_c ft.^{3}/min.	Flow rate Q_i ft.^{3}/min.	Temperature T_c °F	Temperature T_i °F
1.25	18.75	23.40	13.6	27.9	63.8	74.1
			13.3	27.6	64.0	74.1
			14.0	27.6	64.5	74.1
			14.0	27.6	64.6	74.1
			16.0	27.6	66.1	74.1
			16.0	27.2	66.3	74.0
1.35	18.75	25.30	5.5	33.8	55.0	75.4
			5.5	33.8	55.1	75.4
			7.4	33.8	55.1	75.1
			7.7	33.8	55.2	75.1
			9.1	33.4	55.8	75.1
			8.8	33.4	56.0	75.0
			10.5	33.4	57.0	75.0
			10.5	33.8	57.2	75.0
			11.9	33.8	57.8	75.1
			11.6	33.8	58.0	75.2
			13.5	33.8	58.8	75.2
			13.5	33.8	59.0	75.2
			14.6	33.8	59.6	75.3
			14.3	33.8	59.7	75.3
			15.0	33.4	60.2	75.4
			15.0	33.4	60.4	75.4
1.45	18.75	27.20	6.5	38.2	50.7	75.8
			6.5	38.2	50.9	75.9
			7.7	38.2	51.4	76.1
			7.7	38.2	51.4	76.2
			9.8	38.2	52.0	76.3
			9.6	38.2	52.5	76.5
			11.3	38.2	53.5	76.5
			11.0	38.2	53.8	76.6
			12.5	38.2	54.9	76.7
			12.5	38.2	55.2	76.8
			13.5	38.2	56.0	77.0
			13.3	38.2	56.1	77.0
			11.5	38.2	54.3	77.1
			11.5	38.2	54.3	77.1
			9.1	38.2	53.2	77.1
			9.1	38.2	53.0	77.2
			7.5	38.2	52.7	77.2
			7.5	38.2	52.6	77.2
			6.0	38.2	52.0	77.3
			6.0	38.2	52.0	77.3

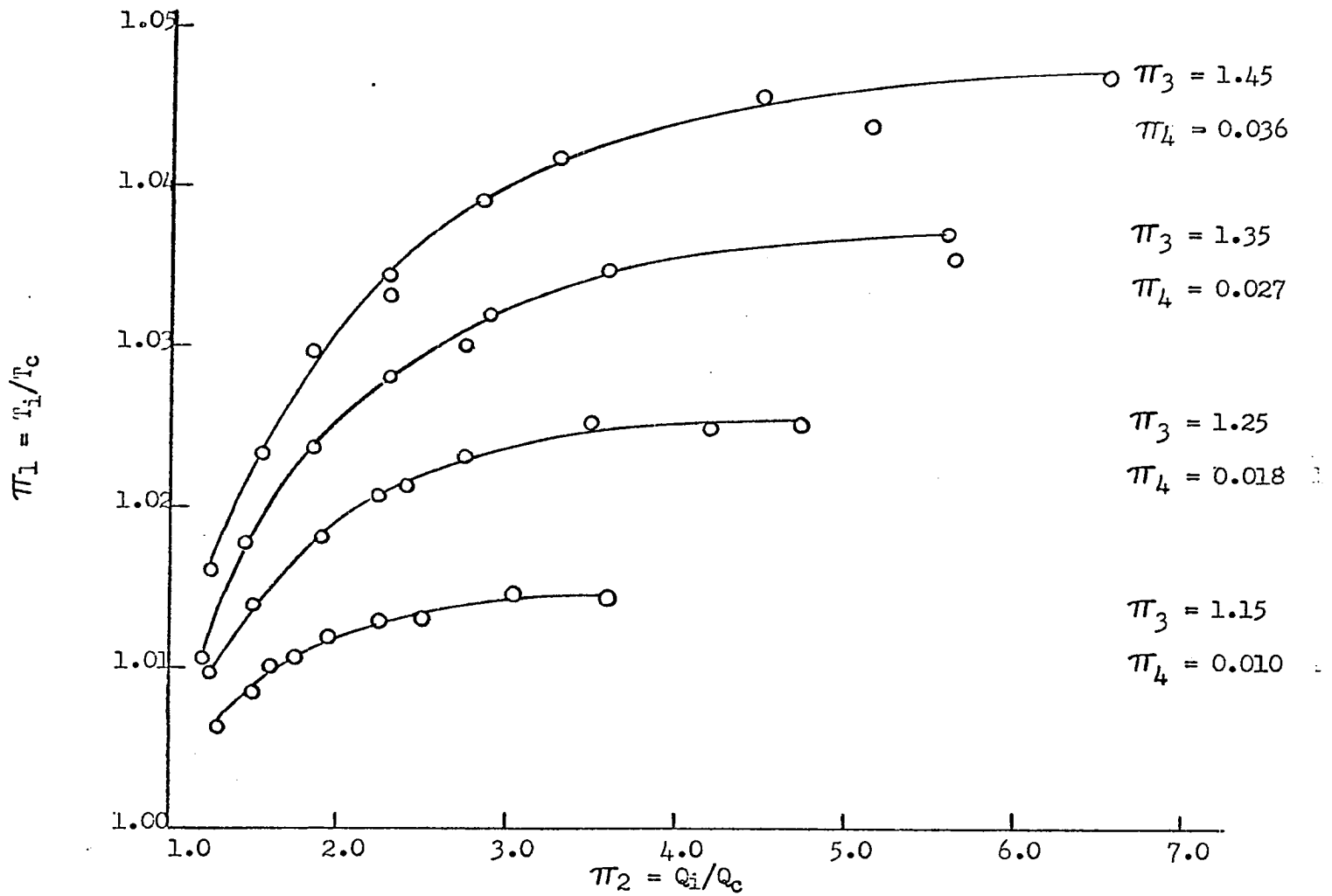

Figure 9. Temperature ratio versus flow ratio. Tube inside diameter = 3/4 inch. High specific humidity. Parameters: $\pi_3 = P_i/P_c$, $\pi_4 = Q_i^2/C_p T_i d_c^4$.

Table 5. Experimental data for Figure 9

Pressure ratio	Pressure P_c psia.	Pressure P_i psia.	Flow rate Q_c ft.^{3}/min.	Flow rate Q_i ft.^{3}/min.	Temperature T_c °F	Temperature T_i °F
1.15	18.58	21.37	3.1	10.4	64.3	72.8
			3.1	10.4	64.7	73.0
			4.0	10.4	65.0	73.1
			4.0	10.1	65.1	73.2
			4.4	10.1	65.5	73.2
			4.4	10.1	65.7	73.2
			5.3	10.1	66.0	73.3
			5.3	10.1	66.1	73.3
			6.1	9.8	66.8	73.3
			6.1	10.1	66.9	73.3
			6.6	9.8	67.4	73.3
			6.6	9.8	67.5	73.3
			9.1	9.8	72.5	73.3
			8.8	9.5	72.5	73.3
			7.7	9.8	70.3	73.4
			7.7	9.8	70.2	73.4
			7.2	9.8	68.4	73.3
			7.2	9.8	68.1	73.3
			5.5	10.1	66.6	73.3
			5.5	9.8	66.5	73.3
			3.7	10.1	65.3	73.3
			3.7	10.4	65.0	73.3
1.25	18.58	23.23	2.8	14.2	58.8	73.2
			2.8	14.5	59.1	73.2
			3.7	14.2	59.1	73.3
			3.7	14.2	59.4	73.3
			4.4	13.8	60.0	73.4
			4.7	14.2	60.2	73.4
			5.3	13.8	60.9	73.4
			5.3	13.8	61.1	73.4
			5.8	13.8	61.2	73.4
			5.8	13.8	61.4	73.4
			6.6	13.8	62.3	73.4
			6.9	13.5	62.4	73.4
			7.4	13.5	63.1	73.4
			7.4	13.5	63.3	73.4
			8.0	13.5	64.0	73.3
			8.0	13.5	64.2	73.3
			8.8	13.5	64.8	73.3
			8.8	13.5	65.0	73.3
			9.8	13.1	66.5	73.3

Table 5 (Continued)

Pressure ratio	Pressure P_c psia.	Pressure P_i psia.	Flow rate Q_c ft.^{3}/min.	Flow rate Q_i ft.^{3}/min.	Temperature T_c °F	Temperature T_i °F
1.25	18.58	23.23	9.8	13.1	66.5	73.3
			10.5	13.1	67.3	73.3
			10.0	12.8	67.4	73.3
			11.2	12.8	70.9	73.2
			11.2	12.8	70.9	73.2
1.35	18.58	25.08	3.3	17.3	53.0	72.5
			3.3	17.3	53.4	72.7
			4.5	17.3	53.6	72.8
			4.5	17.3	53.7	72.8
			5.9	17.0	55.5	72.8
			5.9	17.0	55.7	72.9
			7.5	17.0	57.2	72.9
			7.5	17.0	57.3	72.9
			8.3	17.0	59.0	72.9
			8.3	16.6	59.1	72.9
			9.6	16.6	60.4	73.0
			9.4	16.6	60.7	73.0
			10.8	16.6	62.2	73.0
			10.8	16.6	62.4	73.0
			12.0	16.3	63.7	73.0
			11.7	16.3	63.7	73.0
			13.0	16.0	65.7	73.0
			13.0	16.0	65.7	73.0
			13.5	16.0	67.8	73.0
			13.5	16.0	67.9	73.0
1.45	18.58	26.94	3.6	20.0	48.8	73.1
			3.6	20.0	49.0	73.1
			4.7	20.0	49.7	73.1
			4.5	20.0	50.0	73.1
			6.0	20.0	51.0	73.0
			6.0	20.0	51.2	73.0
			7.3	19.7	52.7	72.9
			7.3	19.7	52.7	72.8
			8.1	19.7	53.9	72.7
			8.1	19.7	54.1	72.7
			10.4	19.7	56.6	72.8
			10.4	19.7	56.8	72.8
			12.2	19.3	59.7	72.8
			12.2	19.3	60.0	72.9
			14.3	18.6	63.0	72.9
			14.0	18.6	63.2	73.0

Table 5 (Continued)

Pressure ratio	Pressure P_c psia.	Pressure P_i psia.	Flow rate Q_c ft.^{3}/min.	Flow rate Q_i ft.^{3}/min	Temperature T_c °F	Temperature T_i °F
1.45	18.58	26.94	12.8	19.3	61.0	73.0
			12.8	19.3	60.9	73.0
			8.8	19.7	56.0	73.1
			8.8	19.7	55.7	73.2
			4.7	20.0	50.7	73.3
			4.7	20.0	50.2	73.3

large as the flow ratio increases. Note also, however, that the temperature ratios tend to limiting values thereby reducing accuracy requirements of the flow ratio and hence, in the author's opinion, these large uncertainties are of no consequence. Figure 11 shows the prediction curves for Figures 5 and 6 and Figures 8 and 9. It may be observed that, while slight differences may be noted from one pressure ratio to another, all curves are within the estimated maximum uncertainty of the prediction factor of the value (see Appendix B):

$$\delta = 1.0 \pm 0.004.$$

The indication of this result is that the distortion of the flow ratio is of little importance. This result is, no doubt, aided by the characteristic of the limiting feature of the temperature ratio.

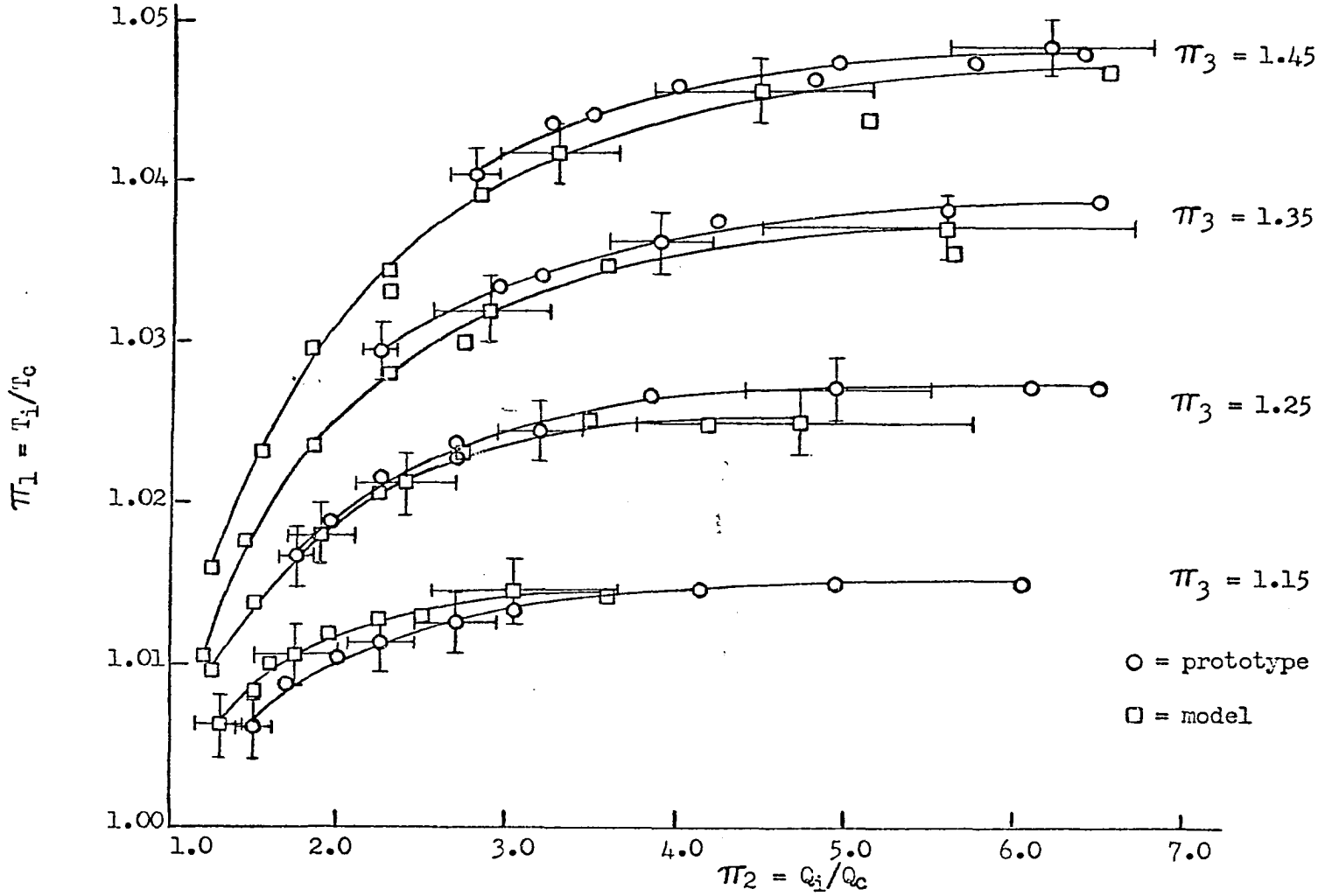

Figure 10. Superposition of prototype (Figure 8) and model (Figure 9). High specific humidity.

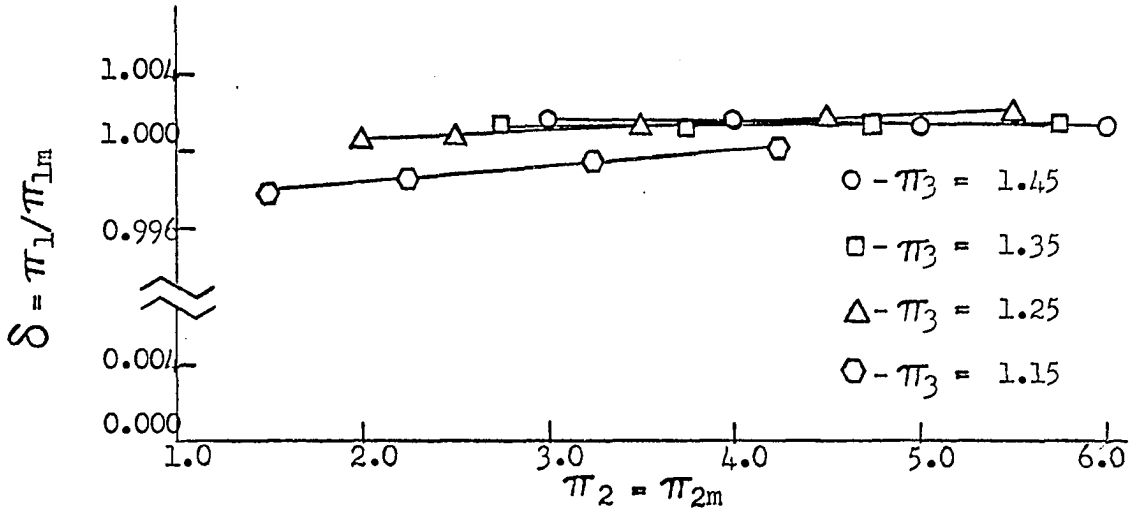

Figure 11a. Prediction factors from Figure 10.

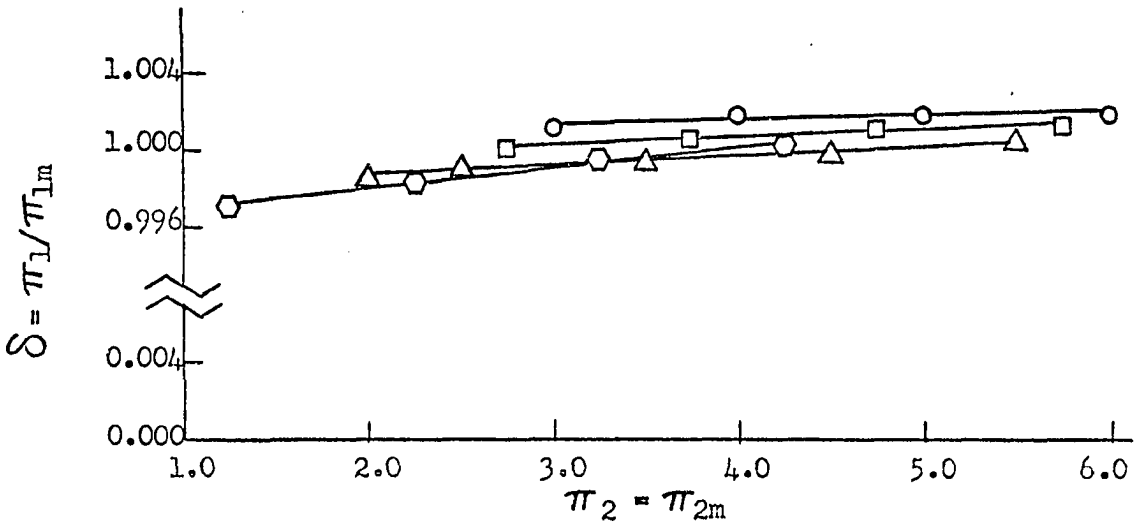

Figure 11b. Prediction factors from Figure 7.

Figure 11. Prediction factors versus flow ratio. Specific humidity and π_4 not considered.

CONCLUSIONS, RECOMMENDATIONS

This work indicates that modeling vortex tubes is not only feasible, but practical. Since the prediction factor is approximately one, the 3/4 inch system may be considered for all practical purposes a true model of the one inch system.

For a given pressure ratio and inlet temperature there is a minimum cold temperature attainable and independent of the flow ratio (above some minimum depending on the pressure ratio) for the range of operation investigated here.

The author recommends additional similitude studies in the following areas:

1. Modeling of vortex tubes with a view to predicting some cooling rate parameter,
2. detailed investigation of the temperature ratio dependence on individual π terms, and
3. extension of the range of the pressure ratio.

LITERATURE CITED

1. Deissler, R. G. and Perlmutter, M. Analysis of the flow and energy separation in a turbulent vortex. International Journal of Heat and Mass Transfer 1: 173-191. 1960.

2. Hilsch, R. The use of the expansion of gases in a centrifugal field as cooling process. Review of Scientific Instruments 2: 108-114. 1947.

3. Hooper, F. C. and Juhasz, I. S. An electric dew point meter cooled by the vortex tube. Refrigerating Engineering 60: 1196-1197. 1952.

4. Keyes, J. J. Experimental study of flow and energy separation in vortex tubes with application to gaseous fission heating. American Rocket Society Journal 31: 1204-1210. 1961.

5. Kuethe, A. M. and Schetzer, J. D. Foundations of Aerodynamics. New York, N.Y., John Wiley & Sons, Inc. c1959.

6. Lay, J. E. An experimental and analytical study of vortex-flow temperature separation by superposition of spiral and axial flows. Journal of Heat Transfer Ser. C, 81: 202-212. 1959.

7. Martynovskii, V. S. and Alekseev, V. P. Investigation of the vortex thermal-separation effect for gases and vapors. Soviet Physics-Tech. Physics 1: 2233-2243. 1956.

8. Murphy, G. Similitude in engineering. New York, N.Y., The Ronald Press Co. c1950.

9. Scheper, G. W., Jr. The vortex tube: internal flow data and a heat transfer theory. Refrigerating Engineering 59: 985-989, 1018. 1951.

10. Shipiro, A. H. Compressible fluid flow. New York, N.Y., The Ronald Press Co. c1953.

11. Sibulkin, M. Unsteady, viscous, circular flow. Part 1. The line impulse of angular momentum. Journal of Fluid Mechanics 11: 291-308. 1961.

12. Sibulkin, M. Unsteady, viscous, circular flow. Part 2. The cylinder of finite radius. Journal of Fluid Mechanics 12: 148-158. 1961.

13. Sibulkin, M. Unsteady, viscous, circular flow. Part 3. Application to the Ranque-Hilsch vortex tube. Journal of Fluid Mechanics 12: 269-293. 1962.

14. Takahama, H. Studies on vortex tubes. Japan Society of Mechanical Engineers Bulletin 8: 433-440. 1965.

15. Vivian, C. H. The Ranque-Hilsch tube. Compressed Air Magazine 68, No. 5: 26-28. 1963.

16. Vortex tube cools protective clothing. Product Engineering 34, No. 20: 27-29. 1963.

17. Westley, R. A bibliography and survey of the vortex tube. Cranfield (England) College of Aeronautics Note No. 9. 1954.

ACKNOWLEDGMENTS

The author takes this opportunity to express his sincere gratitude to his teacher and major professor, Dr. Glenn Murphy, whose advice and assistance were of considerable aid during this work.

The author also wishes to express his sincere appreciation to the Ford Foundation Forgivable Loan Program for the financial assistance which made possible the author's study at Iowa State University.

APPENDIX A. APPARATUS

The apparatus consists of two vortex tubes and test equipment for determining (at the inlet and cold outlet) flow rates, pressures, and temperatures of the air streams.

The values of the length dimensions are given in Table 6 for the vortex tubes.

Table 6. Values of length dimensions

Tube	d_h inch	d_c inch	h inch	w inch	l inch
Prototype	1	1/2	1/4	1/4	24
Model	3/4	3/8	3/16	3/16	12

Two rotameters, each capable of flow measurements of air to 26 SCFM at 14.7 psi and 70°F and designated the Model 10A2235A Ratosight, were obtained from the Fischer-Porter Company, Warminster, Pennsylvania. Since few measurements were actually made at standard pressure, pressure correction curves were also obtained for these instruments.

Four Bourdon - type pressure gauges, two each for measurements to 30 psi and 60 psi and designated Figure No. 23, Catalog No. 26, 1965, were obtained from Marshalltown Gauge, Marshalltown, Iowa.

Three thermometers were employed for determining the inlet and cold outlet temperatures. Their range was -30 to 120°F in 1° calibrations and they were manufactured by Geo. T. Walker and Company, Inc.

APPENDIX B. ERROR ANALYSIS

1. Pressure ratio

$$\text{Max.}\Delta\left(\frac{P_i}{P_c}\right) = \left(\frac{\Delta P_i}{P_i} + \frac{\Delta P_c}{P_c}\right)\left(\frac{P_i}{P_c}\right)$$

By virtue of calibration curves, the uncertainty of the pressure measurements has been reduced to the limit to which they may be read, i.e., 0.1 psi. e.g.,

$$\text{Max.}\Delta\left(\frac{P_i}{P_c}\right) = \left(\frac{0.1}{26.2} + \frac{0.1}{18.7}\right)\left(1.4\right) = 0.0127$$

2. Temperature ratio

$$\text{Max.}\Delta\left(\frac{T_i}{T_c}\right) = \left(\frac{\Delta T_i}{T_i} + \frac{\Delta T_c}{T_c}\right)\left(\frac{T_i}{T_c}\right)$$

The stated accuracy of the thermometers (and verified at the freezing and boiling points of water) is 0.5°F. e.g.,

$$\text{Max.}\Delta\left(\frac{T_i}{T_c}\right) = \left(\frac{0.5}{530} + \frac{0.5}{510}\right)\left(1.0392\right) \approx 0.002$$

3. Flow ratios

$$\text{Max.}\Delta\left(\frac{Q_i}{Q_c}\right) = \left(\frac{\Delta Q_i}{Q_i} + \frac{\Delta Q_c}{Q_c}\right)\left(\frac{Q_i}{Q_c}\right)$$

Rotameters are listed as 2% of full scale or 0.52SCFM. e.g.,

$$\text{Max.}\Delta\left(\frac{Q_i}{Q_c}\right) = \left(\frac{0.52}{20} + \frac{0.52}{10}\right)\left(2\right) = 0.156 \text{ CFM}$$

where 20/10 is to be considered as the flow ratio after the pressure correction has been made.

4. Prediction factor

$$\text{Max.}\Delta\left(\frac{\frac{T_i}{T_c}}{\frac{T_{im}}{T_{cm}}}\right) = \left(\frac{\Delta\left(\frac{T_i}{T_c}\right)}{\frac{T_i}{T_c}} + \frac{\Delta\left(\frac{T_{im}}{T_{cm}}\right)}{\frac{T_{im}}{T_{cm}}}\right)\left(\frac{\frac{T_i}{T_c}}{\frac{T_{im}}{T_{cm}}}\right)$$

$$= \left(\frac{0.002}{1.027} + \frac{0.002}{1.025}\right)\left(1.002\right)$$

$$\approx 0.004$$